



Characterization and Thermal Analysis of Mercury Complexes Containing Intermolecular N→Hg Interactions

HAJAR SAHEBALZAMANI^{§*}, FARSHID SALIMI[§] and SHAHRIARE GHAMMAMY[#]

[§]Departments of Chemistry, Faculty of Science
Ardabil Branch, Islamic Azad University, Ardabil, Iran

[#]Department of Chemistry, Faculty of Science
Islamic Azad University, Malard Branch, Tehran, Iran

sahebalzamanih@yahoo.com

Received 18 February 2011; Accepted 28 April 2011

Abstract: The new mercury (II) compounds with (L¹), (L²) of the general formula [Hg(L)₂], have been synthesized and characterized by elemental analysis, electronic and IR, Raman spectra and thermogravimetry and differential thermogravimetry techniques. The changes observed between the spectra of the ligands and of the complexes allowed us to establish the coordination mode of the metal in complexes and the mechanism of C–H activation is discussed in detail. Thermogravimetry (TG), differential thermal analysis (DTA) and other analytical methods have been applied to the investigation of the thermal behavior and structure of the compounds [Hg(L)₂]. Thermal decomposition of these compounds is multi-stage processes.

Keywords: Organomercury, Hydrazine ligands, Synthesis, Thermal properties

Introduction

Mercury containing ligands *e.g.*, mercuric and mercurous are known to form stable complexes with class b metal ions, such as gold(I)^{1,2} and Se(II)³ because mercury is considered to be a soft Lewis base^{4,5}. The coordination chemistry of transition metals with ligands from the hydrazine family has been of interest due to different bonding modes shown by these ligands with both electron rich and electron poor metals⁶⁻⁸.

The C–H activation obviously depends on both the electron density on the metal and that on the C–H bond that is to be activated, and may be promoted by steric hindrance^{9,10}. The C–H bond is much stronger than the M–C bond and the thermodynamic barrier for homolytic cleavage of a C–H bond is high¹¹. This has opened up its broad synthetic potential and C–H functionalization has become an important topic in organometallic chemistry^{12,13}.

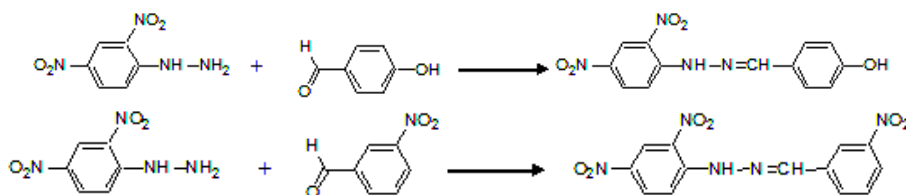
We now report the synthesis the complexes [4-[(2,4-dinitro-phenyl)-hydrazonomethyl]-phenol] Hg(II) (1), [*N*-(2,4-dinitro-phenyl)-*N*-(3-nitro-benzylidene)-hydrazine] Hg(II) (2) and study the role of nitro groups towards metal assisted C–H activation of 2,4-dinitrophenyl hydrazine derivatives¹⁰.

Experimental

All reagents were supplied by Merck and were used without further purification. Melting points were determined using Electrothermal 9200. The Raman spectra were recorded with an Omnac spectrophotometer. The FT-IR spectra were recorded in the range 400–4000 cm⁻¹ by KBr pellet using a Bruker Tensor 27 M 420 FT-IR spectrophotometer. The UV–Vis spectra in CH₃CN were recorded with a WPA bio Wave S2 100 spectrophotometer.

Preparation of Ligands

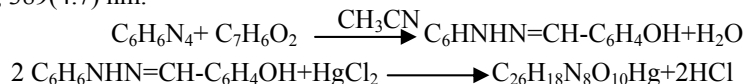
The ligands L¹-L² were dissolved by 2, 4-dinitrophenyl hydrazine (0.39 g, 2 mmol) in 10 mL absolute acetonitrile under temperature 60 °C and addition of this solution derivatives aldehyde (2 mmol dissolved in 5 mL absolute ethanol) was added. The reaction mixture was refluxed for 2 h. After cooling, the precipitate solid was collected, filtered off and finally washed with 5–10 mL cold absolute ethanol and re-crystallized from ethanol (Scheme 1).



Scheme 1. Schematic representation of ligands formation of compounds

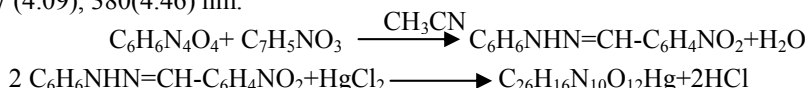
Synthesis of complex [4-[(2,4-Dinitro-phenyl)-hydrazonomethyl]-phenol] Hg(II) [Hg(L¹)₂] (1)

Mercury chloride (1 mmol) was dissolved in absolute acetonitrile (5 mL). To this, (3 mmol) *N*-(2,4-dinitro-phenyl)-*N*-(3-phenyl-allylidene)-hydrazine in DMF (10 mL) was added. The mixture was stirred magnetically at room temperature. The precipitated solid was filtered, washed with H₂O and hexane and then was allowed to stand for 3 d at room temperature whereupon the red solid precipitate was deposited. IR (KBr): 3277(m) cm⁻¹ ν(N-H, str.), 1619(s) cm⁻¹ ν(C=N, str.), 1586(s) cm⁻¹ ν(C-C, str.), 1328(s) cm⁻¹ ν(NO₂ sy, str.), 1216(m) cm⁻¹ ν(N-H in-plane). Raman: 1610 cm⁻¹ ν(C=N, str.), 1580 cm⁻¹ ν(C-C, str.), 1390 cm⁻¹ ν(NO₂ sy, str.), 1280 cm⁻¹ ν(N-H in-plane). UV–Vis (CH₃CN): λ_{max} (log ε): 243(4.41), 281(4.20), 389(4.7) nm.



Synthesis of complex [N-(2,4-Dinitro-phenyl) N-(3-nitro-benzylidene)-hydrazine] Hg(II) [Hg(L²)₂] (2)

Complex (2) was synthesized in a similar manner to that used for complex (1), reacting a mixture of (L²) (3 mmol) and HgCl₂ (1 mmol) in DMF (10 mL). IR (KBr): 3281(m) cm⁻¹ ν(N-H, str.), 1615(s) cm⁻¹ ν(C=N, str.), 1587(s) cm⁻¹ ν(C-C, str.), 1331(s) cm⁻¹ ν(NO₂ sy, str.), 1221(m) cm⁻¹ ν(N-H in-plane). Raman: 1620 cm⁻¹ ν(C=N, str.), 1570 cm⁻¹ ν(C-C, str.), 1380 cm⁻¹ ν(NO₂ sy, str.), 1230 cm⁻¹ ν(N-H in-plane). UV-Vis (CH₃CN): λ max (log ε): 247 (4.28), 277 (4.09), 380(4.46) nm.



Results and Discussion

Elemental analysis data and physical properties are summarized in Table 1. The complexes were prepared in good yield by stirring stoichiometric amounts of HgCl₂ and L¹, L². The complexes are stable in air and light and are soluble in organic solvents such as CHCl₃ and DMSO, less soluble in methanol and insoluble in water and *n*-hexane.

Table 1. The physical and analytical data of the ligands and complexes

Comp. no.	Molecular formula	M. Wt.	Color	M.P °C	Solubility	Elemental Analysis Found (Calc.)		
						%C	%H	%N
L ¹	C ₁₃ H ₁₀ N ₄ O ₅	231	Dark-red	283	DMF	51.65 (51.81)	3.31 (3.28)	18.54 (18.48)
L ²	C ₁₃ H ₉ N ₅ O ₆	207	Orange	297	DMF	47.14 (47.25)	2.74 (2.68)	21.14 (21.20)
1	C ₂₆ H ₁₈ N ₈ O ₁₀ Hg	663	Red	272	DMSO, CHCl ₃	38.87 (38.95)	2.24 (2.19)	13.95 (14.01)
2	C ₂₆ H ₁₆ N ₁₀ O ₁₂ Hg	686	Yellow	285	DMSO, CHCl ₃	36.25 (36.34)	1.85 (1.86)	16.26 (16.31)

IR, Raman spectra

The modes of the coordinated ligands in the complexes have been investigated by means of IR absorption spectra. The presence of electron withdrawing substituents such as a NO₂ group on the aryl ring was regarded to inhibit cyclometallation by rendering the aryl ring as an electrophile, which in turn would have made it unavailable for the attack of an electron deficient metal center¹⁴.

There are some significant changes between the metal(II) complexes and their free ligands for chelation as expected. An exhaustive comparison of the IR spectra of the ligands and complexes gave information about the mode of bonding of the ligands in metal complexes. The IR spectrum of [HgL₂] complexes, the ligands acts as a neutral bidentate through the azomethine nitrogen atom and carbon atom, which is meta to both the NO₂ groups.

The presence of a sharp band at 1586, 1587 cm⁻¹ in IR spectrum and sharp band at 1580, 1570 cm⁻¹ in Raman spectrum, owing to the ν(C-C) (ring) vibrations in the complexes (1), (2) respectively.

In the IR spectra of the complexes a sharp medium band at 1619, 1615 cm⁻¹ in IR spectrum and sharp medium band at 1610, 1620 cm⁻¹ in Raman spectrum owing to the ν(C=N)

(azomethine) vibrations is shifted to lower frequencies in complexes (1), (2) respectively which indicates the use of the azomethine group as one of the coordinating sites of the ligand. The coordination of nitrogen to the metal atom would be expected to reduce the electron density on the azomethine link and thus cause a shift in the C=N band.

In the FT-Raman spectra the N—H in-plane bending vibrations assigned in the region 1280, 1230 cm^{-1} and for the N—H out-of-plane bending falls in the FT-Raman values of 1000–1070 cm^{-1} for the complexes (1), (2) respectively (Figure 1). In the FT-IR spectra the band due to NH stretching in the free ligands occurs in the 3276–3285 cm^{-1} region and remains unaffected after complexation. This precludes the possibility of coordination through the hydrazine nitrogen atom.

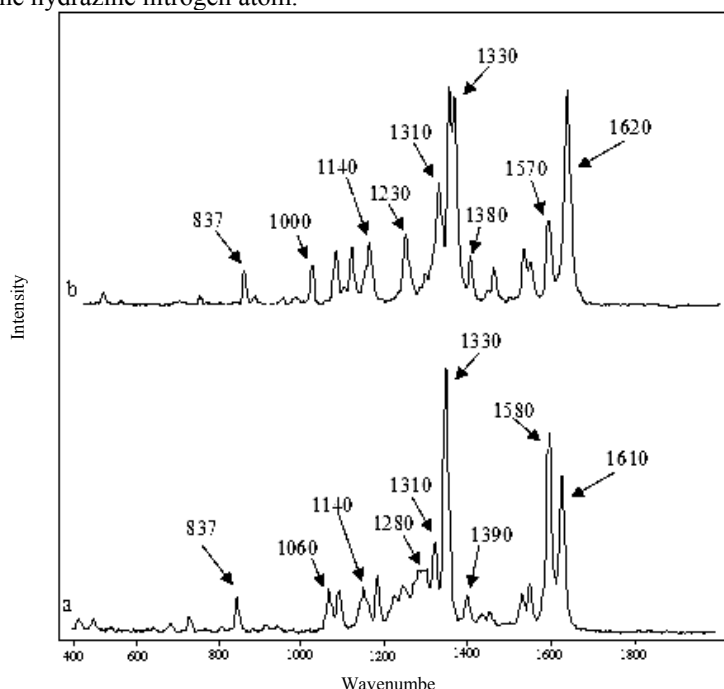


Figure 1. Raman spectra of (a) $[\text{Hg}(\text{L}^1)_2]$, (b) $[\text{Hg}(\text{L}^2)_2]$

The deformation vibrations of NO_2 group contribute to several normal modes in the low frequency region. The medium band at 837 cm^{-1} in FT-Raman spectrum is assignable to NO_2 scissoring mode. Aromatic nitro compounds have medium absorption due to the symmetric stretching vibrations of the NO_2 group at 1390–1310, 1380–1310 cm^{-1} regions in FT-Raman spectrum and in FT-IR spectrum absorption due to the symmetric stretching vibrations of the NO_2 group at 1328, 1331 cm^{-1} in the complexes (1), (2) respectively. The small shift to higher frequency of the band due to $\nu(\text{N}-\text{N})$ can be taken as additional evidence of the participation of the azomethine group in bonding.

Electronic spectra

The formation of the metal(II) complexes was also confirmed by UV-Vis spectra. The UV-Vis solution spectra of the ligands and complexes were also recorded (Figures 2 and 3). When compared complexes with the free ligands values have shifts frequency. All the complexes exhibited three to four bands in the region 243–389 nm. The two absorption bands

appearing in the range 243, 247 and 277, 281 nm may be assigned to a $\pi \rightarrow \pi^*$ transition of the aromatic ring and a $n \rightarrow \pi^*$ transition of the $-\text{C}=\text{N}$ group, respectively. In addition, the low energy absorption peaks in the wavelength range 380–391 nm are associated with a charge transfer transition. The spectra of the complexes do not show any d–d transitions^{15,16}.

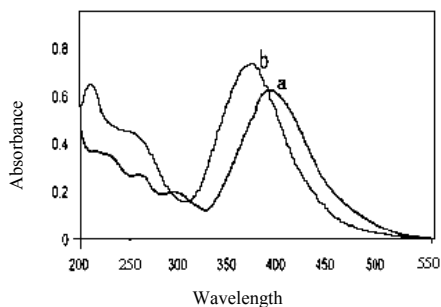


Figure 2. UV-Vis spectra of free ligands (a) L^1 , (b) L^2

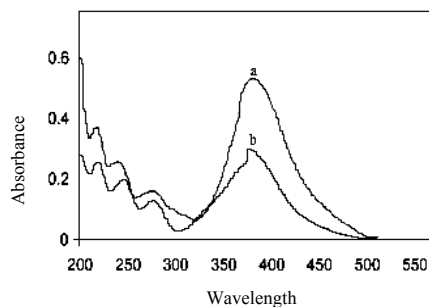


Figure 3. UV-Vis spectra of (a) $[\text{Hg}(L^1)_2]$, (b) $[\text{Hg}(L^2)_2]$

Thermal analysis

The thermal properties of metal(II) complexes were investigated by thermograms (TG, DTG and DTA) and are shown in (Figure 4, 5) and the corresponding thermal analysis data is presented in Table 2.

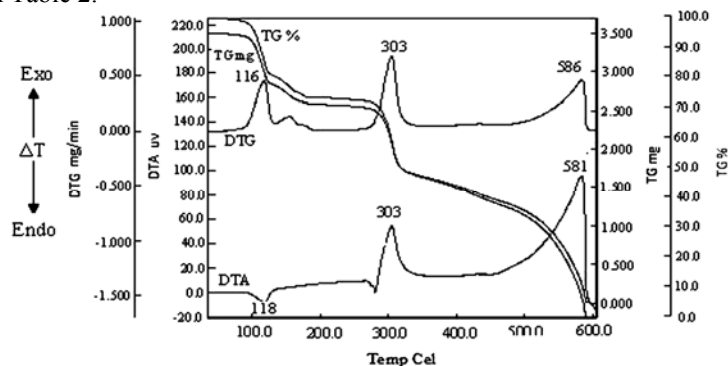


Figure 4. The TG-DTA curves of complex (1)

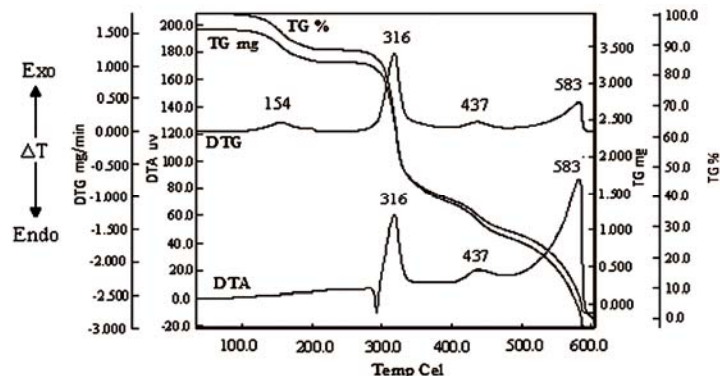


Figure 5. The TG-DTA curves of complex (2)

Table 2. Phenomenological data for the thermal decomposition of the obtained complexes

Complexes	TG results	Stage	DTA results	DTG results	Mass loss, %	
	$T_{\text{rang.}}^{\circ\text{C}}$		$T_{\text{peaks.}}^{\circ\text{C}}$	$T_{\text{peaks.}}^{\circ\text{C}}$	Calculated	Found
1	85-135	1	118 (endo)	116 (exo)	18.33	17.87
	266-325	2	303 (exo)	303 (exo)	23.91	24.39
	488-588	3	581 (exo)	580 (exo)	30.41	31.15
2	110-203	1	-	154 (exo)	11.47	12.15
	279-360	2	316 (exo)	316 (exo)	47.13	47.84
	415-469	3	437 (exo)	437 (exo)	9.42	9.97
	528-590	4	583 (exo)	583 (exo)	23.77	24.32

In the case of complex **(1)** (Figure 4), the decomposition occurs in the 85–588 °C range. There is no mass loss up to 85 °C. The first stage of decomposition starts at 85 °C and ends at 135 °C with a corresponding weight loss 18%, Which is accompanied by endothermic effect in the DTA curve in the range 118 which is accompanied by weight loss confirming. The second stage of decomposition is observed at 266-325 °C (23% wt loss). Meanwhile the DTA curve exhibits exothermic effect in the range 303 °C which is accompanied by weight loss confirming. The three stage of decomposition starts at 488 °C and ends at 588 °C (30% wt loss). The DTA curve exhibits exothermic effect in the range 581 °C which is accompanied by weight loss confirming.

In the case of complex **(2)** (Figure 5), there is no mass loss up to 110 °C. The first stage of decomposition starts at 110 °C and ends at 203 °C with a corresponding weight loss 11%. The second stages of decomposition were observed at 279-360 °C (47% wt loss). Meanwhile the DTA curve exhibits exothermic effect in the range 316 °C which are accompanied by weight loss confirming. The three stage of decomposition was observed at 415-469 °C (9% wt loss). The DTA curve exhibits exothermic effect in the range 437 °C which is accompanied by weight loss confirming. The four stage of decomposition was observed at, 528-590 °C (23% wt loss) for **(2)** complex. The DTA curve exhibits exothermic effect for complex **(2)** in the range 583 °C which is accompanied by weight loss confirming. TGA in air (Figures 4, 5) shows that decomposition with weight loss occurs above 110 °C for complexes **(2)**, which is higher than for complexes **(1)** at 85 °C. Clearly, complex **(2)** has excellent thermal stability.

Conclusion

In this study we have reported the synthesis of new hydrazine derivatives and their Hg(II) complexes. The structural characterizations of synthesized compounds were made by using the elemental analysis, FT-IR and FT-Raman spectroscopy, UV spectral techniques. Thermal properties, TG-DTA of these complexes were studied too. From the spectroscopic characterization, it is concluded that ligands acts as a neutral bidentate through the azomethine nitrogen atom and carbon atom, which is meta to both the NO₂ groups.

References

1. Eikens W, Kienitz C, Jones P G and Thone C A, *J Chem Soc Dalton Trans.*, 1994, 83.
2. Ahmad S, Isab A A, Al-Arfaj A R and Arnold A P, *Polyhedron*, 2002, **21**, 2099.
3. Isab Anvarhusein A, Wazeer Mohammed I M, Fettouhi Mohammed, Ahmad Saeed and Ashraf Waqar, *Polyhedron*, 2006, **25(13)**, 2629-2636.
4. Arnold A P, Tan K S and Rabenstein D L, *Inorg Chem.*, 1986, **25**, 2433-2437.

5. Devillanova F A and Verani G, *Transit Met Chem.*, 1977, **2**, 9.
6. Wang M, Volkert E W, Singh P R, Katti K K, Lusiak P, Katti K V and Barnes C L, *Inorg Chem.*, 1994, **33**, 1184.
7. Katti K V, Reddy V S and Singh P R, *Chem Soc Rev.*, 1995, **24**, 97-107.
8. Katti K V, Singh P R and Barnes C L, *Inorg Chem.*, 1992, **31**, 4588.
9. Abbenhuis H C L, Pfeffer M, Sutter J P, de Cian A, Fischer J, Ji H L and Nelson J H, *Organometallics*, 1993, **12**, 4464.
10. Alsters P L, Engel P F, Hogerheide M P, Copijn M, Spek A L and Koten G van *Organometallics*, 1993, **12**, 1831.
11. Halpern J, *Acc Chem Res.*, 1982, **15**, 238-244.
12. Ryabov A D, Sukharev V S, Alexandrova L, Lagadec R L and Pfeffer M, *Inorg Chem* 2001, **40**, 6529-6532.
13. Matsubara T, Koga N, Musaev D G and Morokuma K, *J Am Chem Soc.*, 1998, **120**, 12692.
14. Cope A C and Friedrich E C, *J Am Chem Soc.*, 1968, **90**, 909.
15. Salib A R, Stefun S L, El-Wafa S M A and El-Shafiy H F, *Synth React Inorg Met Org Chem.*, 2001, **31(5)**, 895.
16. Greaney M A, Coyle C L, Harmer M A, Jordan A and Stifel E I, *Inorg Chem...*, 1989, **28**, 912-920.

